pH Nanosensors

Deutsche Ausgabe: DOI: 10.1002/ange.201509515
Internationale Ausgabe: DOI: 10.1002/anie.201509515

Dimerization of Organic Dyes on Luminescent Gold Nanoparticles for Ratiometric pH Sensing

*Shasha Sun[+], Xuhui Ning[+], Greg Zhang, Yen-Chung Wang, Chuanqi Peng, and Jie Zheng**

Abstract: *Synergistic effects arising from the conjugation of organic dyes onto non-luminescent metal nanoparticles (NPs) have greatly broadened their applications in both imaging and sensing. Herein, we report that conjugation of a well-known pH-insensitive dye, tetramethyl-rhodamine (TAMRA), to pH-insensitive luminescent gold nanoparticles (AuNPs) can lead to an ultrasmall nanoindicator that can fluorescently report local pH in a ratiometric way. Such synergy originated from the dimerization of TAMRA on AuNPs, of which geometry was very sensitive to surface charges of the AuNPs and can be reversely modulated through protonation of surrounding glutathione ligands. Not limited to pH-insensitive dyes, this pH-dependent dimerization can also enhance the pH sensitivity of fluorescein, a well-known pH-sensitive dye, within a larger pH range, opening up a new pathway to design ultrasmall fluorescent ratiometric nanoindicators with tunable wavelengths and pH response ranges.*

Metal nanoparticles (NPs) generally do not fluoresce because of their large density of states; as a result, conjugation of organic dyes to non-luminescent metal NPs is essential for visualizing them in fluorescence imaging systems.[1] For instance, Chan et al. conjugated organic dyes such as Cyto633 to differently sized non-luminescent gold NPs (AuNPs), so that these AuNPs can be readily monitored in real time in vivo.[2] Moreover, this simple approach also creates many synergistic effects that can further broaden imaging and sensing applications of both organic dyes and metal NPs. For example, by loading organic dyes onto plasmonic metal NPs, giant Raman scattering with specific molecular signatures of organic dyes has been used for multispectral cancer imaging.[3] By taking advantage of the fluorescence quenching effect of AuNPs, dye-AuNP complexes can be used as sensors for detecting single-stranded DNA, proteins, and small toxins.[4]

In contrast to conventional non-luminescent metal NPs, a new class of metal NPs that can give intrinsic fluorescence without being labeled with organic dyes has also emerged in the past decade.[5] By tuning particle size, crystallinity, surface ligands, and valance states, we and others were able to create a large number of luminescent metal NPs with tunable emission ranging from UV to NIR.[6] Complementary to dye-labeled non-luminescent metal NPs, metal NPs with intrinsic emissions have also found many applications in imaging and sensing. For instance, red-emitting AuNPs have been used to detect small metal ions, toxin, and reactive oxygen species.[7] More recent studies show that NIR-emitting AuNPs can serve as a new class of renal clearable contrast agents for rapid tumor diagnosis and kidney functional imaging.[8] While the emergence of these luminescent metal NPs suggests that organic dyes might no longer be necessary for detecting metal NPs in the fluorescence imaging systems, whether the conjugation of organic dyes to luminescent AuNPs can create new synergies that neither organic dyes nor luminescent AuNPs possess is still largely unknown and has not been extensively explored.

Herein, we report a reversible ratiometric pH sensing by conjugating a pH insensitive dye, 581 nm emitting TAMRA (Supporting Information, Figure S1), onto pH-insensitive near-infrared (NIR)-emitting glutathione-coated AuNPs (GS-AuNPs; Figure 1 A). When the pH increased from 6 to 10, the emission intensity of TAMRA increased over five-fold while the emission intensity of GS-AuNPs only changed less than 10 %. Thus, the emission ratio of TAMRA to GS-AuNP was found to linearly depend on the pH of the local environment. Photophysical spectroscopic studies show that this pH-dependent emission of TAMRA originates from its dimerization on the AuNPs, of which the geometry was highly sensitive to the protonation of glutathione on AuNPs. Not limited to pH-insensitive dyes, a well-known pH-sensitive dye, fluorescein, became even more sensitive to pH changes within a larger pH range after being conjugated to GS-AuNPs. These results clearly indicate that this unique enhancement arising from conjugation of organic dyes onto luminescent AuNPs offers a pathway to design ultrasmall ratiometric pH-responsive nanoindicators.

Synthesis of TAMRA conjugated GS-AuNPs (TG-AuNPs) was very straightforward. We synthesized 815 nm emitting GS-AuNPs with a reported method before[8a] and then incubated NHS-TAMRA (1.6 μM) with GS-AuNPs (0.4 nM) in phosphate buffered saline (PBS) solution in the dark at room temperature. After 24 h, unreacted pink colored TAMRA was removed with a sephadex column and a reddish-colored solution was collected. The conjugation of TAMRA onto GS-AuNPs was first confirmed by agarose gel electrophoresis. As shown in Figure 1 B, while yellowish GS-AuNPs (lane 1) and free pinkish TAMRA (lane 3) have distinct motilities, reddish-colored TG-AuNPs (lane 2) have a mobility similar to that of GS-AuNPs. High-resolution transmission electron microscopy (HR-TEM) showed that the average diameter of the TG-AuNPs is 2.2 ± 0.4 nm (Figure 1 C), consistent with the core size (2.1 ± 0.5 nm) of GS-

[*] S. Sun,[+] X. Ning,[+] G. Zhang, Y. Wang, C. Peng, Prof. Dr. J. Zheng
Department of Chemistry, The University of Texas at Dallas
800 W. Campbell Rd., Richardson, TX 75080 (USA)
E-mail: jiezheng@utdallas.edu

[+] These authors contributed equally to this work.

Supporting information for this article is available on the WWW under http://dx.doi.org/10.1002/anie.201509515.

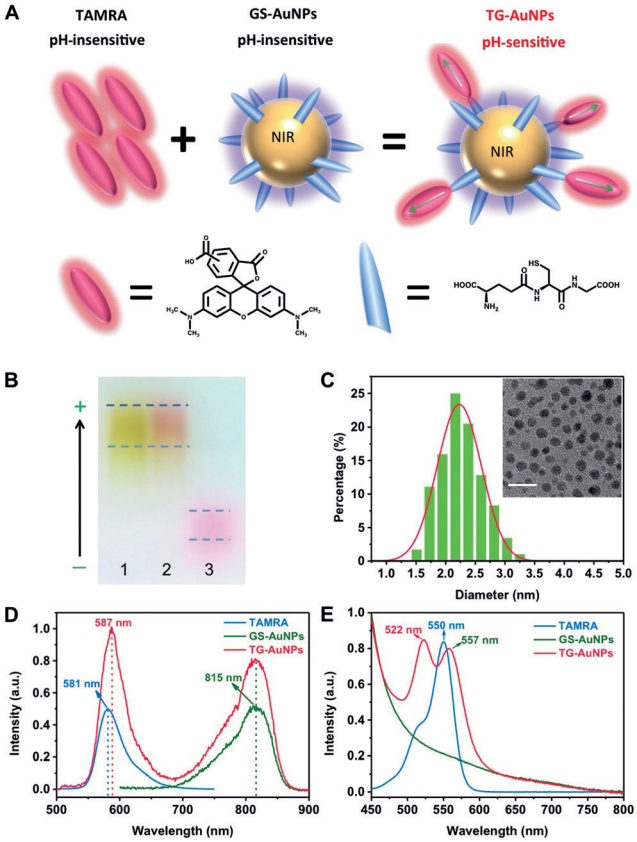

Figure 1. A) Illustration of the conjugation of pH-insensitive tetramethyl-rhodamine (TAMRA) onto pH-insensitive GS-AuNPs. B) Agarose gel electrophoresis of GS-AuNPs (1), TG-AuNPs (2), and TAMRA (3). C) HR-TEM image and size distribution of TG-AuNPs. Scale bar = 10 nm. D) Emission spectra of TAMRA, GS-AuNPs, and TG-AuNPs collected at 350 nm excitation. E) Absorption spectra of TAMRA, GS-AuNPs, and TG-AuNPs.

AuNPs.[8a] The average number of TAMRA on one GS-AuNP was found to be about 4 (Supporting Information).

While AuNPs are known to partially quench fluorescence of organic dyes on their surface,[9] fluorescence spectra of TG-AuNPs showed that dual-colored emissions were still observed and centered at 587 nm and 815 nm under 350 nm excitation, corresponding to the emissions of TAMRA dyes and GS-AuNPs, respectively (Figure 1D; Supporting Information, Figure S2). Compared to the emission maximum (581 nm) of free monomeric TAMRA in aqueous solution, a 6 nm red shift in the emission of TAMRA after being conjugated onto GS-AuNPs implies dipole–dipole couplings among TAMRA molecules on AuNPs,[10] which was further confirmed by their UV/Vis absorption. As shown in Figure 1E, free TAMRA exhibited a strong absorption peak at 550 nm. An additional small shoulder peak at 522 nm was due to association between monomeric TAMRA molecules in aqueous solution.[11] After the conjugation to GS-AuNPs, the strong absorption at 550 nm was split into two peaks: one peak was located at 522 nm and the other was red-shifted to 557 nm, consistent with previous reports[12] on dimerization of TAMRA molecules, further confirming dipole–dipole couplings of TAMRA dimers on GS-AuNPs. Because both blue and red shifts in absorption of TAMRA were observed, according to well-known molecular excitation coupling theory,[12a] the dimers of TAMRA are not parallel to each other but have intermediate geometries.[13]

While both monomeric TAMRA and GS-AuNPs are insensitive to pH changes from 6 to 10 (Figure 2A), TAMRA

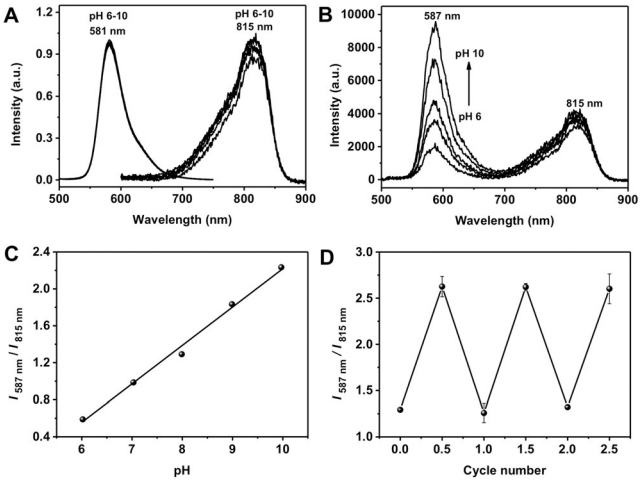

Figure 2. A) Fluorescence spectra of TAMRA and GS-AuNPs at different pH values. B) Fluorescence spectra of TG-AuNPs at different pH values. C) The relationship between pH and $I_{587\,nm}/I_{815\,nm}$ ratio. D) Reversibility of fluorescence intensity ratios ($I_{587\,nm}/I_{815\,nm}$) of TG-AuNPs with pH change between 6 and 10.

exhibited strong pH-dependent emission after being conjugated onto GS-AuNPs. As shown in Figure 2B, with the increase of the pH value from 6 to 10, the fluorescence intensity at 587 nm gradually increased more than 5-times while the emission intensity from the GS-AuNPs changed less than 10% in this range. Thus, the intensity ratio of the two emissions became linearly dependent of pH (Figure 2C). Such dependence is highly reversible. As shown in Figure 2D, by repeatedly switching pH from 6 to 10, very little variation was observed in the ratio, which is distinct from irreversible pH sensors derived from micelle or avidin loaded with TAMRA[11,14] and other known ratiometric pH indicators.[15] The pH response of TG-AuNPs was still independent of the concentration (Figure S3), indicating the changes in the fluorescence intensity at different values were not induced by the aggregation of AuNPs. It should be noted that further decrease of the pH below 5 induced partial aggregation of TG-AuNPs, limiting their pH applications in more acidic environments.

To fundamentally understand the pH response mechanism of TAMRA on GS-AuNPs, we further investigated UV/Vis absorption of TG-AuNPs at pH 6 and 10, respectively. As shown in Figure 3A, with the decrease of pH from 10 to 6, the absorption peak at 522 nm showed very little red shift (0.6 nm) while the absorption peak at 556 nm was red-shifted to 561 nm. This suggested that the pH did not significantly affect head-to-head coupling between transition dipoles of dimers; however, it did significantly strengthen the head-to-tail coupling between transition dipoles. These changes also

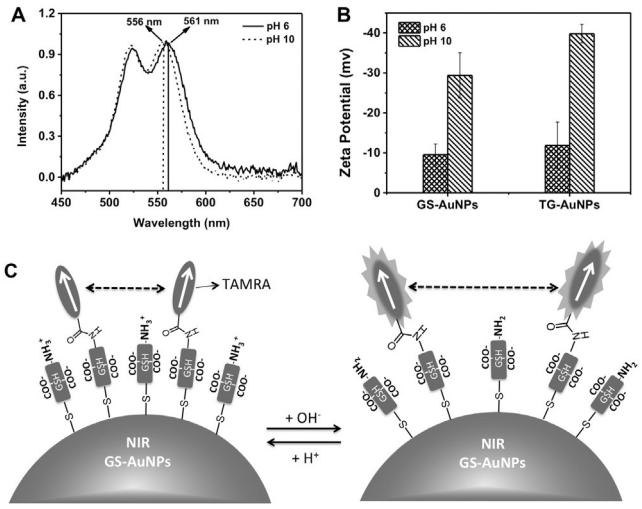

Figure 3. A) Absorption spectra of TAMRA on TG-AuNPs at pH 6 and pH 10, respectively. B) Zeta potentials of GS-AuNPs and TG-AuNPs at pH 6 and pH 10, respectively. C) A hypothesized pH responsive mechanism of TG-AuNPs.

implied that the angle between two transition dipoles became larger and the couplings were weakened with increasing pH.[13] Therefore, energy transfer between TAMRA dimers became less efficient and emission of TARMA dramatically increased.[12a,b,13] On the other hand, 810 nm emission of GS-AuNPs shows very little pH response (< 10 %), similar to pure GS-AuNPs, implying little fluorescence resonance energy transfer between TAMRA and GS-AuNPs. This result is consistent with our fluorescence lifetime measurements. The average lifetime of 810 nm emission from pure GS-AuNPs was measured to be 1.39 ± 0.08 μs, nearly identical to that (1.19 ± 0.05 μs) from TG-AuNPs, indicating no fluorescence energy transfer between TAMRA and GS-AuNPs (Figure S4).

To further understand the origin of the pH effect on the dimerization of TAMRA on GS-AuNPs, we measured the zeta potentials of TG-AuNPs at pH 10 and 6. As shown in Figure 3B, with the decrease of pH from 10 to 6, the overall zeta potential of TG-AuNPs was reduced by about −20 mV (from −39.8 mV to −11.8 mV), almost identical to the zeta potential change (from −29.4 mV to −9.5 mV) of pure GS-AuNPs.[16] The reduction in zeta potential is attributed to the protonation of amine group of GS-AuNPs rather than TAMRA because TG-AuNPs and pure GS-AuNPs showed an almost identical trend. More detailed studies on zeta potential of TG-AuNPs at different pH conditions showed that the decrease of pH resulted in gradual reduction on the overall surface charge of TG-AuNPs owing to protonation of amine group of glutathione (Figure S5). The observed gradual decrease in the surface charges owing to protonation of amine group of glutathione immobilized on the AuNPs is consistent with recent reports on pK_a changes of these ligands after being immobilized on NP surface.[17] Combining the UV/Vis absorption, fluorescence, and zeta potentials of TG-AuNPs at different pH environments, a hypothesized mechanism was proposed in Figure 3C: with the increase of pH from 6 to 10, the angle between transition dipoles of TAMRA dimers on GS-AuNPs was slightly increased and the couplings of TAMRA dimers was reduced owing to the increased repulsion among negatively charged GSH ligands on the AuNPs. Thus, the fluorescence intensity of TAMRA would dramatically increase with pH increase.

To investigate whether the observed reversible pH-dependent dimerization can be applied to pH-sensitive dyes, we conjugated 5(6)-carboxyfluorescein (Figure S6), a well-known pH-sensitive dye,[18] onto GS-AuNPs using the same method (Supporting Information). The average size of fluorescein-conjugated GS-AuNPs (FG-AuNPs) is 2.2 ± 0.5 nm (Figure 4A), similar to TG-AuNPs. After subtracting

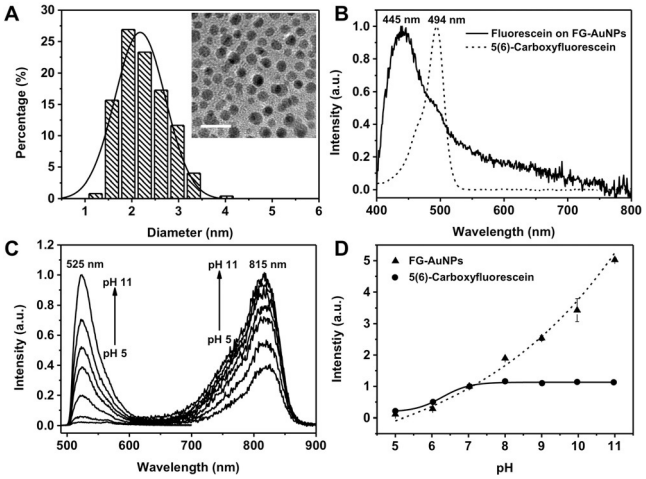

Figure 4. A) HR-TEM image and size distribution of FG-AuNPs. Scale bar = 10 nm. B) Absorption spectra of 5(6)-carboxylfluorescein and 5(6)-carboxylfluorescein on FG-AuNPs. C) Fluorescence spectra of FG-AuNPs excited at 350 nm and 470 nm for 810 nm and 525 nm emissions, respectively. D) Normalized fluorescence intensity of FG-AuNPs and 5(6)-carboxylfluorescein at 525 nm.

the absorption of GS-AuNPs, a new peak at 445 nm was observed from FG-AuNPs, 47 nm blue-shifted compared to the absorption maximum of free fluorescein (Figure 4B) and consistent with the previous report (40 nm) on H-dimerization of fluorescein.[19]

A much more sensitive pH-dependent emission was observed in FG-AuNPs. When the pH is increased from 5 to 11, the 525 nm emission intensity of fluorescein on AuNPs under 470 nm excitation had increased about 19 times (Figure 4C); it was nearly 4 times more sensitive to pH than that of free fluorescein in the same pH window (Figure 4D). Furthermore, unlike free fluorescein that only responded to pH change in the range of 5 to 7 (Figure S7), the emission of fluorescein on AuNPs remained pH-responsive until the pH reached 11. More interestingly, 815 nm emission of AuNPs after fluorescein conjugation (under 350 nm excitation; Figure S8) became sensitive to pH changes: as the pH increases from 5 to 11, the 815 nm emission increased about 3.5 times. This difference between TG-AuNPs and FG-AuNPs is likely due to the more efficient energy transfer between fluorescein emission and GS-AuNPs excitation, resulting from a larger spectral overlap (47 % more; Figure S9). To further confirm

energy transfer between fluorescein and GS-AuNPs, we also measured the lifetimes of 810 nm emission from GS-AuNPs before and after conjugation with fluorescein, and found that the lifetime of 810 nm decreased from 1.39 ± 0.08 μs to 0.81 ± 0.05 μs (Figure S10), distinct from the observation of TG-AuNPs (Figure S4), further confirming energy transfer between fluorescein and GS-AuNPs. Moreover, the FG-AuNPs can also report pH in a ratiometric way (Figure S11).

In summary, conjugation of organic dyes to ultrasmall luminescent AuNPs leads to a unique enhancement that enables pH-insensitive dyes to exhibit pH-dependent emission and pH-sensitive dyes to become more sensitive to pH changes in a larger pH range. Therefore, the emission ratio of organic dyes and AuNPs can be used to quantitatively report local pH changes. Such intriguing pH responses originate from the dimerization of organic dyes on the ultrasmall AuNP surface, of which geometries were found to be very sensitive to surface charges and can be modulated through the protonation of surrounding AuNP surface ligands. It should be noted that such pH-dependent emission is limited to ultrasmall AuNPs because we no longer observed similar pH-dependent emission from TAMRA on the 7 nm TG-AuNPs surface, even though TAMRA emission was still observed (Figure S12). Nevertheless, this synergistic effect resulted from simple conjugation of organic dyes to ultrasmall luminescent AuNPs, and opens new pathways to design fluorescent ratiometric nanoindicators with tunable emission wavelengths and a broad pH-responsive range.

Acknowledgements

The authors would like to thank Xinya Jiang and Jing Xu for their assistance in lifetime measurements and pH adjustment. This work was supported by the NIH R01DK103363, CPRIT RP140544, TexasMRC award, and the start-up fund from The University of Texas at Dallas (J.Z.)

Keywords: dimerization · dyes · gold nanoparticles · luminescence · pH sensors

How to cite: *Angew. Chem. Int. Ed.* **2016**, *55*, 2421 – 2424
Angew. Chem. **2016**, *128*, 2467 – 2470

[1] a) J. Xie, K. Chen, J. Huang, S. Lee, J. H. Wang, J. Gao, X. G. Li, X. Y. Chen, *Biomaterials* **2010**, *31*, 3016 – 3022; b) M. Palner, K. Pu, S. Shao, J. Rao, *Angew. Chem. Int. Ed.* **2015**, *54*, 11477 – 11480; *Angew. Chem.* **2015**, *127*, 11639 – 11642; c) X. Hu, X. Gao, *ACS Nano* **2010**, *4*, 6080 – 6086.

[2] L. Y. T. Chou, W. C. W. Chan, *Adv. Healthcare Mater.* **2012**, *1*, 714 – 721.

[3] X. M. Qian, X. H. Peng, D. O. Ansari, Q. Yin-Goen, G. Z. Chen, D. M. Shin, L. Yang, A. N. Young, M. D. Wang, S. M. Nie, *Nat. Biotechnol.* **2008**, *26*, 83 – 90.

[4] a) B. Dubertret, M. Calame, A. J. Libchaber, *Nat. Biotechnol.* **2001**, *19*, 680 – 681; b) M. Swierczewska, S. Lee, X. Y. Chen, *Phys. Chem. Chem. Phys.* **2011**, *13*, 9929 – 9941.

[5] a) J. Zheng, J. T. Petty, R. M. Dickson, *J. Am. Chem. Soc.* **2003**, *125*, 7780 – 7781; b) J. Zheng, C. Zhang, R. M. Dickson, *Phys. Rev. Lett.* **2004**, *93*, 077402; c) J. Zheng, P. R. Nicovich, R. M. Dickson, *Annu. Rev. Phys. Chem.* **2007**, *58*, 409 – 431.

[6] a) C. Zhou, G. Y. Hao, P. Thomas, J. B. Liu, M. X. Yu, S. S. Sun, O. K. Oz, X. K. Sun, J. Zheng, *Angew. Chem. Int. Ed.* **2012**, *51*, 10118 – 10122; *Angew. Chem.* **2012**, *124*, 10265 – 10269; b) C. Zhou, M. Long, Y. P. Qin, X. K. Sun, J. Zheng, *Angew. Chem. Int. Ed.* **2011**, *50*, 3168 – 3172; *Angew. Chem.* **2011**, *123*, 3226 – 3230; c) J. Zheng, C. Zhou, M. Yu, J. Liu, *Nanoscale* **2012**, *4*, 4073.

[7] a) H. Wei, Z. Wang, L. Yang, S. Tian, C. Hou, Y. Lu, *Analyst* **2010**, *135*, 1406 – 1410; b) T. T. Chen, Y. H. Hu, Y. Cen, X. Chu, Y. Lu, *J. Am. Chem. Soc.* **2013**, *135*, 11595 – 11602.

[8] a) J. B. Liu, M. X. Yu, X. H. Ning, C. Zhou, S. Yang, J. Zheng, *Angew. Chem. Int. Ed.* **2013**, *52*, 12572 – 12576; *Angew. Chem.* **2013**, *125*, 12804 – 12808; b) M. X. Yu, J. B. Liu, X. H. Ning, J. Zheng, *Angew. Chem. Int. Ed.* **2015**, *54*, 15434 – 15438; *Angew. Chem.* **2015**, *127*, 15654 – 15658; c) M. Y. Yu, J. Zheng, *ACS Nano* **2015**, *9*, 6655 – 6674.

[9] E. Dulkeith, A. C. Morteani, T. Niedereichholz, T. A. Klar, J. Feldmann, S. A. Levi, F. van Veggel, D. N. Reinhoudt, M. Moller, D. I. Gittins, *Phys. Rev. Lett.* **2002**, *89*, 203002.

[10] F. Del Monte, J. D. Mackenzie, D. Levy, *Langmuir* **2000**, *16*, 7377 – 7382.

[11] M. Ogawa, N. Kosaka, C. A. S. Regino, M. Mitsunaga, P. L. Choyke, H. Kobayashi, *Mol. Biosyst.* **2010**, *6*, 888 – 893.

[12] a) O. Valdes-Aguilera, D. C. Neckers, *Acc. Chem. Res.* **1989**, *22*, 171 – 177; b) M. Ogawa, N. Kosaka, P. L. Choyke, H. Kobayashi, *ACS Chem. Biol.* **2009**, *4*, 535 – 546; c) H. Kobayashi, M. Ogawa, R. Alford, P. L. Choyke, Y. Urano, *Chem. Rev.* **2010**, *110*, 2620 – 2640.

[13] K. Adachi, K. Watanabe, S. Yamazaki, *Ind. Eng. Chem. Res.* **2014**, *53*, 13046 – 13057.

[14] K. Zhou, Y. Wang, X. Huang, K. Luby-Phelps, B. D. Sumer, J. Gao, *Angew. Chem. Int. Ed.* **2011**, *50*, 6109 – 6114; *Angew. Chem.* **2011**, *123*, 6233 – 6238.

[15] a) G. T. Hanson, R. Aggeler, D. Oglesbee, M. Cannon, R. A. Capaldi, R. Y. Tsien, S. J. Remington, *J. Biol. Chem.* **2004**, *279*, 13044 – 13053; b) . Kurishita, T. Kohira, A. Ojida, I. Hamachi, *J. Am. Chem. Soc.* **2010**, *132*, 13290 – 13299; c) A. M. Dennis, W. J. Rhee, D. Sotto, S. N. Dublin, G. Bao, *ACS Nano* **2012**, *6*, 2917 – 2924.

[16] M. X. Yu, C. Zhou, J. B. Liu, J. D. Hankins, J. Zheng, *J. Am. Chem. Soc.* **2011**, *133*, 11014 – 11017.

[17] D. Wang, R. J. Nap, I. Lagzi, B. Kowalczyk, S. Han, B. A. Grzybowski, I. Szleifer, *J. Am. Chem. Soc.* **2011**, *133*, 2192 – 2197.

[18] J. Han, K. Burgess, *Chem. Rev.* **2010**, *110*, 2709 – 2728.

[19] I. L. Arbeloa, *J. Chem. Soc. Faraday Trans.* **1981**, *77*, 1725 – 1733.

Received: October 11, 2015
Revised: December 14, 2015
Published online: January 8, 2016

